Polymers with Strongly Interacting Groups: Theory for Nonspherical Multiplets

A. N. Semenov,* I. A. Nyrkova, and A. R. Khokhlov

Physics Department,† Moscow State University, Moscow 117234, Russia

Received November 15, 1994; Revised Manuscript Received July 17, 1995⊗

ABSTRACT: A general theory for microstructure in systems of copolymers with strongly interacting groups (SIGs) is proposed. The so-called superstrong segregation limit, corresponding to rather short blocks containing SIGs and strong attraction between them, is considered in detail. In particular, multiplet formation in melts and solutions of ionomers (block ionomers) is studied. It is shown that as the interaction parameter increases, the most stable shape of a multiplet continuously changes from spherical to disklike (oblate ellipsoid). A further increase of the interaction parameter induces another (first order) transition from disklike multiplets to lamellae. The same transitions could be induced by decreasing the average length of ionic blocks in block ionomer systems. The relevant experimental observations are discussed.

1. Introduction

Polymeric systems with strongly interacting groups (SIGs) include block copolymers, ionomers, and associating polymers. Intensive attention paid to all these systems in recent years[1−34] is connected in particular with various microdomain (micellar, multiplet) structures inherent to the systems. Most research has been carried out in the field of microphase separation and micellar formation in block copolymer systems, in particular, in diblock copolymer melts.[2,17−24,29−31,35,36]

In all these systems microdomain formation is forced by an effective incompatibility (immiscibility) of the components of polymer chains. For example, in melts of A−B diblock copolymers unlike blocks (A and B) tend to separate if the effective Flory parameter $\chi = \chi_{AB} - 0.5(\chi_{AA} + \chi_{BB})$ is positive, which is normally the case. In solutions of ionomers or associating polymers, it is soluble and insoluble (strongly attracting) chain fragments that effectively repel each other and thus separate and form multiplet structures.

The physical reasons leading to microdomain formation suggest that general properties of systems with strongly interacting groups could be understood in a framework of a common general theory. In particular, the ideas and approaches developed in the area of microphase separation of block copolymers can also be used (with minor modifications) to describe the behavior of systems of ionomers and associating polymers. This program has been initiated in ref 37, where a strong similarity between an ionomer chain (Figure 1a) and a multiblock copolymer with strongly asymmetric composition (Figure 1b) has been discussed.

Ionic groups (as well as hydrophobic groups in associating polymer solutions) usually strongly attract each other. Thus we should expect that the most characteristic regime for ionomer systems corresponds to the strong segregation limit (SSL)[17−24] in block copolymer terminology. More importantly, it was shown[37] that in fact ionomer systems are likely to fall in a novel superstrong segregation limit (sSSL), which can also be realized in systems of block copolymers with strong incompatibility and compositional asymmetry.

The aim of the present contribution is to extend the previous theory[37] in two directions: (1) to investigate the formation of nonspherical microdomains (micelles, multiplets) which have also been observed in experiments[11−16] and (2) to consider not only melts but also solutions of polymers with SIGs. As a main result of this paper, we show that it is nonspherical disk-shaped multiplets that are most characteristic for copolymers in the superstrong segregation regime.

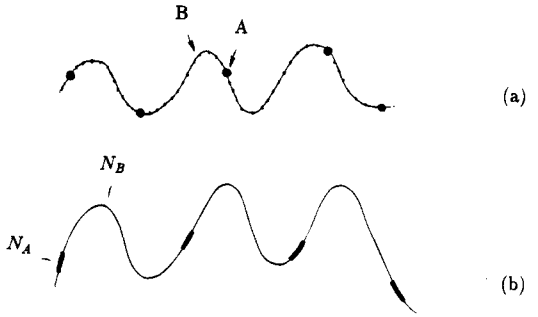

Figure 1. (a) Ionomer; (b) multiblock copolymer, $N_A \ll N_B$.

The model and the basic theories for strong and superstrong segregation regimes are briefly described in the next section. Sections 3 and 4 are devoted to the theory of nonspherical micelles in melts and in solutions of polymers with SIGs. The results are compared with available experimental data in the last section.

2. The Model and Strong and Superstrong Segregation.

2.1. The Model. Let us consider a system of multiblock copolymer chains (see Figure 1b). Each chain is a sequence of short A blocks (N_A links per block) and long B blocks (N_B links per block, $N_B \gg N_A$). The number of blocks per chain is assumed to be very large (this assumption is not crucial and can be easily lifted). The B fragments are assumed to be flexible:

$$\sigma_B \sim a_B^2$$

where σ_i is the effective cross-section of an i block, a_i is the corresponding statistical length, i = A, B. The volume per link is $v_i = \sigma_i a_i$ (note that here we consider a link as a section of polymer chain with contour length equal to the statistical length, and effective link thus defined is not identical to a chemical link, although normally the difference is not large). The rms end-to-end distance between the ends of an unperturbed (Gaussian) i block is $R_i = a_i N_i^{0.5}$.

† E-mail: sasha@ppl.phys.msu.su.

⊗ Abstract published in *Advance ACS Abstracts,* September 1, 1995.

0024-9297/95/2228-7491$09.00/0

We assume that A links are asymmetric and are larger than B links:[38]

$$a_A^3 \gg v_A = \sigma_A a_A; \qquad \sigma_A \gg \sigma_B; \qquad a_A \gg a_B \sigma_A/\sigma_B \quad (1)$$

We also assume that B blocks are long enough:

$$N_B v_B \gg N_A v_A \quad (2)$$

We will consider multi-(AB) chains both in the melt state and in a selective solvent which is good for B blocks and is extremely poor for A blocks. The melt considered in the current and in the next sections is assumed to be incompressible.

Interactions between the links in the melt state are characterized by the effective incompatibility parameter χ, which is assumed to be large enough: $\chi N_A \gg 1$. The last condition implies that the effective energy of attraction between A blocks is much larger than kT; it is normally valid for ionomers and block ionomers where attraction between A links is due to dipole–dipole interaction.[39]

Note that extremely short A blocks, $N_A = 1$, correspond to a regular ionomer,[3-5] whereas $N_A > 1$ corresponds to a block ionomer.[6-8] Since the last case is more general, we will assume it below; the results derived can be also (at least qualitatively) applied to normal ionomers ($N_A = 1$).

2.2. Micelles in the Strong Segregation Limit. Strong energy of attraction between A blocks dictates that at equilibrium they must separate and form aggregates, or micelles in the block copolymer language or multiplets in the ionomer case (Figure 2a). Since the composition is strongly asymmetric ($N_B \gg N_A$), the shape of the micelles is expected to be spherical.[22,24-28] The condition $\chi N_A \gg 1$ ensures that the segregation is strong: unlike (B) links cannot penetrate into aggregates, which are characterized by narrow sharp interfaces.[17-24] The equilibrium size R of an A aggregate (core of a micelle) is determined by the balance between the interfacial free energy and the conformational free energy of A and B blocks inside the core and the corona. A large energy of attraction between A links implies that the interfacial tension, γ, is also large. This favors larger micelles (with smaller interfacial area per block). Therefore the blocks must be highly stretched in the core and partly in the corona regions: the conformational free energy is basically the elastic energy of this stretching.[22]

The characteristics of micelles in SSL have been quantitatively considered in detail.[22,26-28] Here we briefly review the main approach. The free energy of a micelle can be written as a sum of three terms:

$$F = F_{intf} + F_{core} + F_{corona} \quad (3)$$

where $F_{intf} = 4\pi R^2\gamma$ is the free energy of the interface, F_{core} is the elastic free energy of A blocks, and F_{corona} is the free energy of elastic stretching of B blocks. The interfacial tension γ can be calculated analytically under certain conditions;[21] here we treat γ as a known parameter which could be large due to strong incompatibility between unlike links (in particular, $\gamma\sigma_A$ could be much larger than kT).

The number of A blocks per aggregate, Q, is determined by its size via simple geometry:

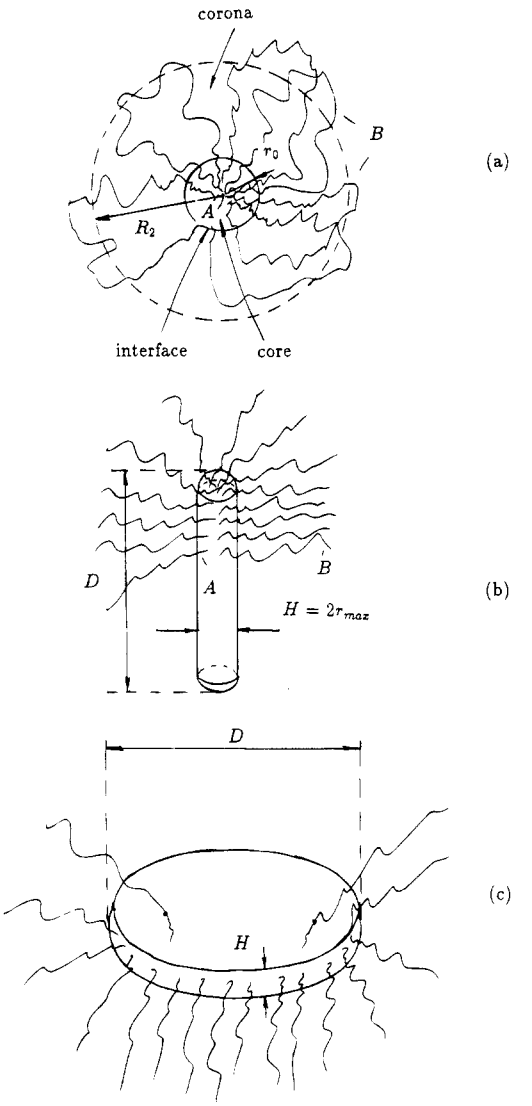

Figure 2. (a) Spherical micelle: a core of radius R is surrounded by the corona filled by B loops. The size of the corona, R_2, is much larger than R. In the superstrong segregation limit, $R \to R_{max} = H/2$, where $H = N_A a_A$. (b) A cylindrical aggregate of thickness $H = 2R_{max}$ and total length D. (c) Disklike aggregate: the total diameter = D, and the thickness = H. In all cases micellar coronas are nearly spherical.

$$Q = \frac{4\pi}{3}\frac{R^3}{N_A v_A} \quad (4)$$

The core free energy can be estimated as (in kT units)

$$F_{core} \sim Q\frac{R^2}{N_A a_A^2} \quad (5)$$

where $R^2/(N_A a_A^2)$ is of the order of the energy of elastic stretch of an A block along the radius, R. The energy of the corona can be estimated in a similar way;[22] the result is

$$F_{corona} \sim \frac{v_B}{a_B^2}\frac{Q^2}{R}$$

so that

$$F_{corona} \sim F_{core}\left(\frac{v_B a_A^2}{v_A a_B^2}\right) \quad (6)$$

The inequality (1) ensures now that $F_{corona} \gg F_{core}$; the core contribution is thus neglected in what follows.

In order to calculate F_{corona}, we note that B blocks are always less stretched than A blocks. In fact, even when the A blocks are completely stretched (i.e., the core radius, R, is of order $N_A a_A$), the degree of stretching of B fragments is small: $d_s \lesssim \sigma_B/\sigma_A \ll 1$ (see the first inequality (1)), where d_s is the ratio of the typical end-to-end distance of a fragment of a B block relative to the contour length of the fragment. Thus the stretched fragments of B blocks in a corona are characterized by nearly ideal (Gaussian) elasticity. It is also important to note that the corona volume, V_B, is much larger than that of the core, V_A (see eq 2):

$$V_B/V_A = (N_B v_B)/(N_A v_A) \gg 1$$

Hence the corona size $R_2 \sim V_B^{1/3}$ is much larger than the core radius:

$$R_2/R \sim \left(\frac{N_B v_B}{N_A v_A}\right)^{1/3} \gg 1 \quad (7)$$

The two conditions specified above (large corona size and ideal elasticity of B blocks inside it) ensure the validity of an electrostatic analogy[22] between the micellar corona and the electric field of a certain charged system. The analogy implies that the averaged vector connecting neighboring chain links, $\mathbf{dr}(n)/dn$ (here $\mathbf{r}(n)$ is the position of the nth link of a chain), formally corresponds to an electric field, $\mathbf{E}$. The electrostatic energy $(1/8\pi)\int E^2\, d^3r$ is thus proportional to the energy of elastic stretching of B blocks, F_{corona}. Also a coarse-grained (smoothed) trajectory of a B block should correspond to an electric force line which therefore must break at an AB junction point. Hence the charged system can be constructed by attributing a unit charge to each junction point located near the core/corona interface. The elastic free energy of the corona is then just proportional to the total energy of the electric field outside the core. Thus for a spherical interface, we get[22]

$$F_{corona} = \frac{C}{2}\frac{Q^2}{R} \quad (8)$$

where

$$C = \frac{3}{4\pi}\frac{v_B}{a_B^2} \quad (9)$$

is the polymer/electrostatic proportionality constant.

The equilibrium radius of a micelle and the number of blocks per micelle can now be obtained by minimization of the free energy per block, $F/Q \simeq (F_{intf} + F_{corona})/Q$. The results are[22,37]

$$R = \left[\frac{3}{4}\frac{a_B^2}{v_B}\gamma(N_A v_A)^2\right]^{1/3} \quad (10)$$

$$Q = \pi\gamma N_A v_A a_B^2/v_B \quad (11)$$

The above analysis based on the SSL limit is valid provided that the typical energy per block is large (in kT units): $F/Q \gg 1$. Using eqs 3 and 8–11, the last condition can be rewritten as

$$\gamma \gg \gamma_{min} = a_B\left(\frac{1}{v_A v_B N_A}\right)^{1/2} \quad (12)$$

Note that the condition (12) is weak if N_A is large enough. Note also that the conditions (1) and (12) imply that the number of blocks per micelle is large, $Q \gg 1$.

2.3. Superstrong Segregation Limit. It is natural to assume that the value of the interface tension (in kT/σ_B units) increases as temperature is decreased. In turn, an increase of γ induces an increase of micellar size (see eq 10). At some large enough $\gamma = \gamma^*$, the core radius can formally (according to eq 10) exceed the value $N_A a_A/2$, the half-length of a completely stretched A block. Obviously, this situation is virtually impossible since such a large radius implies that the central part of the core must be empty, which is physically very unfavorable. It is important to note that even if the core radius, R, is close to the limiting value $R_{max} = N_A a_A/2$, our expressions for the corona and interface free energies still remain valid. Therefore the predictions, eqs 10 and 11, are quantitatively valid in the whole region $\gamma_{min} \ll \gamma < \gamma^*$, where γ^* is determined by the condition $R(\gamma^*) = R_{max}$.[37]

$$\gamma^* = \frac{1}{6}\frac{N_A a_A^3 v_B}{v_A^2 a_B^2} \quad (13)$$

In the region $\gamma > \gamma^*$, which was called the superstrong segregation (sSSL) region in ref 37, the micellar size is constant: $R = R_{max}$, $Q = (\pi/6)(N_A^2 a_A^3/v_A)$. In the sSSL regime all A blocks are strongly stretched in the radial direction, some of them being almost completely stretched hairpins (of length $N_A a_A/2$).

As was pointed out,[37] the superstrong segregation is difficult to access in the block copolymer case since γ^* is proportional to N_A; however, this regime must be characteristic for ionomers and associative polymers since for these systems the typical interfacial tension, γ, is large and N_A (which is proportional to the size of the ionic or associating group) is relatively small.[40]

3. Nonspherical Micelles in Copolymer Melts

The aggregates (cores of micelles) attain their limiting size R_{max} at the beginning of the sSSL regime considered in the previous section. An aggregate cannot grow further while retaining spherical shape as this growth would imply the creation of a very unfavorable empty hole in its central region. The formal geometrical restriction is that the minimum distance between any point inside an aggregate and its surface must be not exceed R_{max}. It is easy to see that aggregates can still grow in one or two dimensions while obeying this restriction.

In both cases they would become nonspherical as a result: in the first case, they tend to become cylinders of radius R_{max} (Figure 2b), and in the second, disks of thickness $H = 2R_{max}$ (Figure 2c). The corresponding transitions are analyzed below.

3.1. Sphere to Disk Transition. The micellar free energy, F, in a general case can be calculated just in the same way as for a spherical micelle. In particular, the core contribution, F_{core}, can still be neglected in comparison with F_{corona}, provided that conditions (1) are fulfilled. Thus,

$$F \simeq F_{\text{intf}} + F_{\text{corona}} \tag{14}$$

where the first term is just proportional to the interfacial area, S: $F_{\text{intf}} = \gamma S$, and the corona contribution can be defined using the electrostatic analogy described above.

To simplify our task a bit, we assume that an aggregate can be either a sphere–cylinder (a cylinder with two half-spherical caps; see Figure 2b) or a disk with a rounded edge (see Figure 2c). Both shapes can be obtained by rotation of a rectangle of height H and width $D - H$ with two half-circles of diameter H adjoined to its sides around the vertical (to get a disk) or horizontal (cylinder) symmetry axis.

The volume of a disklike aggregate is

$$V = \frac{\pi}{6}H^3 + \frac{\pi^2}{8}H^2(D - H) + \frac{\pi}{4}H(D - H)^2 \tag{15}$$

where D is its total diameter and $H = N_A a_A$ is its thickness. The corresponding interfacial free energy is

$$F_{\text{intf}} = \pi\gamma\left[H^2 + \frac{\pi}{2}H(D - H) + \frac{1}{2}(D - H)^2\right] \tag{16}$$

We now need to calculate the elastic free energy of the corona. Let us start with the disk in the limit $D \gg H$. Here the corona free energy is proportional to the electrostatic energy of a uniformly charged thin disk:

$$F_{\text{corona}} = Ck_{\text{form}}\frac{Q^2}{D} \tag{17}$$

where $k_{\text{form}} = 16/(3\pi)$ is the disk form factor and C is given by eq 9.

Note that eq 17 is in agreement with the analogous result[41] in the limit $R_2 \gg D \gg H$ (see eq 22 of ref 41). We stress however that our result, eq 17 with $k_{\text{form}} = 16/(3\pi)$, which was obtained using the electrostatic analogy, is exact in the specified limit, whereas eq 22 of ref 41 was obtained using additional approximations which lead to a different numerical prefactor. However, the numerical difference is not important: it is about 3%.

In the general case, the form factor, k_{form}, is a function of the disk asymmetry, H/D. In order to calculate the function $k_{\text{form}}(H/D)$, we use an additional approximation and substitute for the disk a conducting oblate ellipsoid with the same diameter and the same volume; thus the lengths of the axes are

$$l_x = l_y = D; \qquad l_z \equiv h = \frac{6V}{\pi D^2}$$

With this approximation, we find[42]

$$k_{\text{form}}(H/D) = \frac{\arctan[(D^2/h^2 - 1)^{1/2}]}{(1 - h^2/D^2)^{1/2}} \tag{18}$$

Equation 18 is obviously exact for $D = H$ (spherical micelle); it underestimates the exact result ($k_{\text{form}} = 16/(3\pi)$ for $D \gg H$ by only 7%. We thus conclude that eq 18 provides a good approximation for a disk form factor.

The volume of a cylindrical aggegate is

$$V = \frac{\pi}{12}H^2(3D - H) \tag{19}$$

Note that now D is the total length of the cylinder, and $H = N_A a_A$ is its thickness. The free energy of the aggregate can be calculated in just the same way as for the case of disks. The interfacial contribution is

$$F_{\text{intf}} = \pi\gamma HD \tag{20}$$

The corona part of the free energy is given by eq 17 with

$$k_{\text{form}}(H/D) = \frac{\ln[D/h + (D^2/h^2 - 1)^{1/2}]}{(1 - h^2/D^2)^{1/2}} \tag{21}$$

The form factor, eq 21, was calculated using as an approximation a conducting prolate ellipsoid of the same length D and the same volume. The thickness of the ellipsoid is thus

$$h = \left(\frac{6V}{\pi D}\right)^{1/2}$$

It can be easily shown that eq 21 is asymptotically exact in both limits $D = H$ (sphere) and $D \gg H$ (long uniformly charged cylinder).

In order of find the equilibrium characteristics of a micelle, we must minimize the micellar free energy per block, F/Q, where F is defined by eqs 14–21, $Q = V/(N_A v_A)$ is the total number of (A) blocks inside an aggregate, and V is the total volume of the aggregate, which depends on D and H (see eqs 15 and 19). As a result, we show that the spherical micelles are stable in the whole strong segregation region $\gamma_{\min} < \gamma < \gamma^*$. On the other hand, in the superstrong segregation regime, $\gamma > \gamma^*$, the spherical shape readily becomes unstable: instability with respect to both oblate and prolate deformations occurs at $\gamma = \gamma^*$. In the region $\gamma > \gamma^*$ the free energy minimum always corresponds to a disklike shape; thus at equilibrium cylindrical aggregates should never appear.

Note that by definition D is always larger than H (or equal H). As $D = H$ corresponds to a spherical shape, we can consider the difference, $s = D - H$, as an order parameter for the sphere to disk transition. The general Landau-like expansion of the free energy (per chain) as a series in s in the vicinity of the transition point is

$$F/Q \simeq C_0 + C_1(\gamma^* - \gamma)s + C_2 s^2 + \ldots$$

where it is easy to check that both constants C_1 and C_2 are positive. Therefore the minimum of the free energy corresponds to $s = 0$ (spherical shape) if $\gamma < \gamma^*$ and to $s \simeq (C_1/2C_2)(\gamma - \gamma^*)$ if γ is slightly higher than γ^*. Thus we arrive at a special kind of a second-order transition, which is characterized by a nearly linear dependence of the order parameter $(D - H)$ on $\gamma - \gamma^*$ in the vicinity of the transition point $\gamma = \gamma^*$. The whole dependence of the aggregate diameter, D, on the interfacial tension γ (in the region $\gamma > \gamma^*$) was calculated numerically; within 3% accuracy it can be approximated by a simple equation

$$D = H + \frac{2}{3}H[(\gamma/\gamma^*)^{1/2} - 1] \tag{22}$$

Thus the diameter of an aggregate increases as γ is increased; in the limit $\gamma \gg \gamma^*$ the dependence obeys the 0.5 power law:

$$D = 2\left(\frac{2}{3}\right)^{1/2}H\frac{v_A a_B}{a_A^{1.5} v_B^{0.5}}\left(\frac{\gamma}{N_A}\right)^{1/2} \tag{23}$$

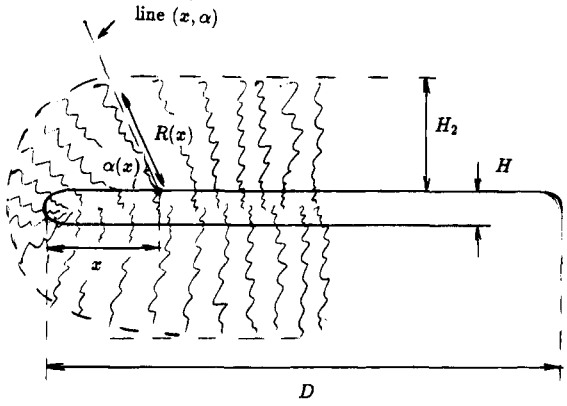

Figure 3. A disk in the regime $D \gg H_2$, where H_2 is the average corona thickness. Near the edge the B blocks are tilted; the length of a block "grafted" to the disk at the distance x from the edge is $R(x)$, the angle between its trajectory and the disk surface being $\alpha(x)$.

3.2. Disks vs Infinite Sheets. The above treatment, and in particular the electrostatic analogy, is valid provided that the characteristic corona size, R_2, is much larger than the core size, D. Note that the above condition implies that the corona is nearly spherical even if the core is strongly asymmetric. This condition is automatically satisfied for a spherical micelle (see eq 7) since $N_B v_B \gg N_A v_A$. This is not the case, however, for disklike aggregates. Using the incompressibility of the melt, we get $R_2^3 \sim QN_B v_B$; using also eqs 22, we obtain

$$R_2/D \sim \left[\frac{N_B v_B}{N_A v_A}\left(\frac{\gamma^*}{\gamma}\right)^{1/2}\right]^{1/3}$$

Therefore at $\gamma \sim \gamma^* [(N_B v_B)/(N_A v_A)]^2$ the corona size becomes of the order of the micellar diameter and our approximations fail. It is natural to assume that in the region $\gamma > \gamma^{**} \sim \gamma^*[(N_B v_B)/(N_A v_A)]^2$ the aggregate diameter becomes larger than the corona thickness. In this case the corona becomes a nearly planar B brush uniformly (apart from the edge region) grafted to the disk surfaces (Figure 3). The thickness of the corona, H_2, is again determined by the incompressibility condition:

$$H_2 = \left(\frac{N_B v_B}{N_A v_A}\right)\frac{H}{2} \tag{24}$$

(note that $H_2 \gg H$).

A detailed analysis (see below) shows that in fact a first-order transition from disklike aggregates to the aggregates in the form of infinite planar sheets (lamellae) occurs in the region $\gamma \sim \gamma^{**}$. In order to approximately locate this transition, let us write the free energy of a strongly asymmetric micelle, $D \gg H_2$ (see Figure 3) as

$$F \simeq \text{const} \times Q + \pi D(\tilde{F}_{intf} + \tilde{F}_{corona}) \tag{25}$$

where const does not depend on the diameter D and the second term on the right-hand side represents the edge correction to the free energy. Here πD is the edge length, and $\tilde{F} = \tilde{F}_{intf} + \tilde{F}_{corona}$ is the correction per unit edge length; $\tilde{F}$ nearly does not depend on D in the region $D \gg H_2$.

The equilibrium micellar structure (in particular, equilibrium diameter) should correspond to the minimum of the free energy per block

$$F/Q = \text{const} + \frac{\pi D}{Q}\tilde{F} \tag{26}$$

Taking into account that $Q \sim D^2$, we thus arrive at minimization of $\tilde{F}/D$. Obviously, the minimum corresponds to $D \to \infty$ (infinite sheet) if $\tilde{F}$ is positive. This is surely the case if γ is large enough since $\tilde{F}_{intf}$ is proportional to γ and $\tilde{F}_{corona}$ nearly does not depend on γ (see below). Therefore the transition from disks to lamellae is approximately specified by the condition

$$\tilde{F} \equiv \tilde{F}_{intf} + \tilde{F}_{corona} = 0 \tag{27}$$

A further comment concerning the type of the transition is relevant at this point. For $\tilde{F} = 0$ the approximate equation (26) does not predict any dependence of the free energy per block on the disk diameter. To get this dependence (assuming that D is large), we need to take into account that the edge energy is slightly dependent on D due to a curvature of the disk edge: $\tilde{F} = \tilde{F}(D)$. The corresponding correction to $\tilde{F}_{intf}$ is proportional to H/D, whereas a correction to $\tilde{F}_{corona}$ is proportional to H_2/D and thus dominates since $H_2 \gg H$. Note that the corona free energy with a curved edge is lower than that for a straight edge (i.e., in the limit $D \to \infty$): any curvature implies that B blocks near the edge have more free space. Therefore we can write $\tilde{F} = \tilde{F}(\infty) - C_1(H_2/D)$, where $\tilde{F}(\infty)$ is the limiting value of the edge energy and $C_1 > 0$ is a constant which does not depend on D. Hence eq 26 can be rewritten as

$$F/Q \simeq \text{const} + \frac{\pi D}{Q}\left(\tilde{F}(\infty) - C_1\frac{H_2}{D}\right) = \text{const} + \frac{K_0}{D} - \frac{K_1}{D^2} \tag{28}$$

where K_0 and K_1 are again constants and we take into account that $Q \propto D^2$. Equation 28 is valid if $D \gg H_2$; it implies that infinite sheets ($D \to \infty$) are not favorable if $\tilde{F}(\infty) < 0$. For $\tilde{F}(\infty) > 0$ this equation generally implies two minima: for $D = \infty$ and for a finite D. Therefore we predict a first-order transition between disks of finite diameter and infinite sheets at some particular positive value of $\tilde{F}(\infty)$, which corresponds to γ slightly higher than that defined by eq 27, where the effect of edge curvature was neglected.

The calculation of $\tilde{F}_{intf}(\infty)$ is straightforward: it is just proportional to the interface area excess associated with the edge,

$$\tilde{F}_{intf} = \frac{\pi}{4}\gamma H \tag{29}$$

In order to calculate the corona contribution to the edge effect, $\tilde{F}_{corona}(\infty)$ (for zero edge curvature), we need to consider conformations of B blocks near the disk edge in more detail. Far from the edge (at distances larger than H_2), the B blocks are stretched normal to the disk surface, the thickness of the corona, H_2, being given by eq 24. Note that H_2 is still much smaller than the contour length of a B block, $N_B a_B$; i.e., the degree of stretching of B blocks in the corona is well below the limiting value. Near the edge the corona thickness is decreasing, and the blocks are tilted, so that the angle α between a block trajectory and the disk surface depends on the distance from the edge, x (see Figure 3).

At this point we introduce two assumptions concerning the conformations of B blocks. First we assume that the B blocks are all stretched in a similar way (the

Alexander approximation[43]); the elastic free energy calculated with this approximation is known to be valid within 20% accuracy.[22] We also assume that the trajectories of the B blocks are straight lines on the average even in the region where they are tilted.

Thus the conformation of B blocks is determined by the two functions $\alpha(x)$ and $R(x)$, the latter being the length of the blocks starting at the distance x from the edge (see Figure 3). These functions are connected via the incompressibility condition:

$$\frac{d\alpha}{dx} = \frac{2}{R^2}(H_2 - R\sin(\alpha)) \tag{30}$$

where H_2 is defined by eq 24. Obviously, $R \to H_2$ and $\alpha \to \pi/2$ far from the edge (for $x \gg H_2$).

The elastic free energy per half-block can now be calculated in a standard way:[22,37]

$$F_{el} = \frac{3}{2a_B^2}\int_0^{N_B/2}\left(\frac{dr}{dn}\right)^2 dn = \frac{3}{2a_B^2}\int_0^{R(x)}\left(\frac{dr}{dn}\right) dr$$

where $r(n)$ is the average distance between the junction point and the nth link of a B block (starting at a given distance x from the edge). The function dr/dn is again determined by the incompressibility condition (see refs 22 and 37 for more detail).

Let us consider a strip on the disk surface of thickness Δx. The number of functional (A) blocks per unit length of the strip, $\Delta Q = \Delta x/\sigma_A$, obviously coincides with the number of stretched halfs of B blocks starting in the same interfacial area. These B blocks must tightly fill the corona region between the line (x, α) shown in Figure 2 and a similar line $(x + \Delta x, \alpha + \Delta\alpha)$. The number of links per half of a B block at the distances between r and $r + \Delta r$ from the corresponding junction point is $\Delta n = \Delta r/(dr/dn)$. The total volume of all links in the corresponding subregion, $v_B\Delta n\delta Q$, must coincide with the volume of this subregion, $\Delta V = \Delta r(\Delta x \sin\alpha + r\Delta\alpha)$. Therefore $v_B(dn/dr)(\Delta x/\sigma_A) = \Delta x \sin\alpha + r\Delta\alpha$. Taking now the limit $\Delta x \to 0$, we get

$$\frac{dr}{dn} = \frac{v_B}{\sigma_A}\left(\sin(\alpha) + r\frac{d\alpha}{dx}\right)^{-1}$$

Using the last two equations, we get the elastic free energy of the corona per unit area of the disk surface:

$$\mathcal{F}_{el} \equiv F_{el}/\sigma_A = \frac{3v_B a_A^2}{2a_B^2 v_A^2}\left(\frac{d\alpha}{dx}\right)^{-1}\ln\left(1 + R\frac{d\alpha}{dx}\sin^{-1}(\alpha)\right) \tag{31}$$

Apparently, $\mathcal{F}_{el}$ is tending to $\mathcal{F}_{el}^{\infty} = [(3v_B a_A^2)/(2a_B^2 v_A^2)] \times H_2$ for $x \gg H_2$. Obviously, the total edge correction is

$$\tilde{F}_{corona} = 2\int_0^{\infty}(\mathcal{F}_{el} - \mathcal{F}_{el}^{\infty})\, dx \tag{32}$$

where the factor "2" accounts for two surfaces (upper and bottom) of a disk core and ∞ stands for D since the integral on the right-hand side is expected to be convergent in the characteristic region $x \sim H_2 \ll D$. Using now eqs 30–32, we obtain

$$\tilde{F}_{corona} = K\int_0^{\pi/2}\frac{0.5\varrho^2}{1 - \varrho\sin(\alpha)} \times \left[\frac{0.5\varrho^2}{1 - \varrho\sin(\alpha)}\ln\left(\frac{2}{\varrho\sin(\alpha)} - 1\right) - 1\right] d\alpha \tag{33}$$

where

$$K = 3v_B\left(\frac{N_B\sigma_B}{2\sigma_A^2}\right)^2$$

and $\varrho = R(x)/H_2$ can also be considered as an unknown function of α.

Minimization of the right-hand-side of eq 33 with respect to $\varrho(\alpha)$ results in

$$\tilde{F}_{corona} \simeq -0.50K = -\frac{3}{8}v_B\left(\frac{N_B\sigma_B}{\sigma_A^2}\right)^2 \tag{34}$$

Equation 34 is in agreement with the results for the corona edge energy in disklike rod–coil copolymer micelles,[44] which were obtained using a somewhat different approach.[45]

Using the function $\varrho(\alpha)$ determined by the minimization and eq 30, we obtain the dependencies $R(x)$ and $\alpha(x)$. In particular, we get the asymptotic behavior for $x \gg H_2$

$$\alpha(x) = \frac{\pi}{2} - \text{const} \times \exp\left(-\frac{3}{2}\frac{x}{H_2}\right)$$

which ensures that the edge effect is exponentially small for inner parts of the disk.

Substituting eqs 29 and 34 into eq 27, we locate the transition from disklike micelles to lamellae at

$$\gamma^{**} \simeq \frac{3}{2\pi}\frac{v_B\sigma_B^2}{v_A\sigma_A^3}\frac{N_B^2}{N_A} \tag{35}$$

Note that

$$\frac{\gamma^{**}}{\gamma^*} = \frac{36}{\pi}\left(\frac{N_B v_B}{N_A v_A}\right)^2 \gg 1$$

Thus γ^{**} is proportional to N_B^2; it must therefore be very high if B blocks are very long (N_B is very large); the transition to infinite lamellae is probably inaccessible for these systems.

The core diameter at the transition point, D^{**}, can still be approximately defined by eq 23. The result is

$$\frac{D^{**}}{H} = \frac{4}{\pi^{1/2}}\frac{v_B N_B}{v_A N_A} \tag{36}$$

Thus the geometrical asymmetry of micelles at the transition point is directly determined by the compositional asymmetry of multiblock copolymers. The different regimes considered above are summarized schematically in the diagram of Figure 4. The dependence of the diameter, D, of an aggregate (a micellar core) on interfacial tension γ is shown in Figure 5 on a log–log scale.

4. Nonspherical Micelles in Solutions

Let us turn to a solution of multiblock copolymer chains of the type considered above. The solvent is assumed to be good for the major (B) component and extremely poor for the other (A) component. Thus A blocks effectively attract each other and tend to separate and form aggregates (micelles) as in the melt system. We will consider the structure of the micelles for a very dilute solution where a single-chain approximation is

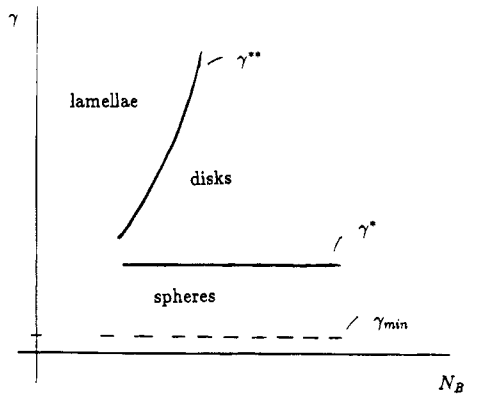

Figure 4. Different multiplet geometries indicated on a schematic phase diagram. The region between γ_{min} and γ^* corresponds to the strong segregation limit; $\gamma > \gamma^*$ corresponds to superstrong segregation.

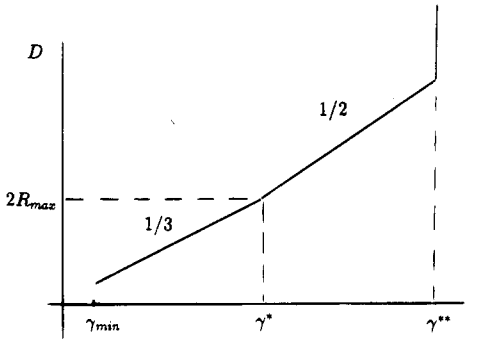

Figure 5. Log–log plot of the diameter D of an aggregate vs interfacial tension γ.

valid. Let us first assume that the aggregates (cores of micelles) are spheres of radius R.

4.1. Spherical Micelles. The free energy of a micelle can again be represented as a sum of three terms, eq 3. The core of a micelle is densely packed by A links; therefore the core and the interfacial contributions to the free energy are the same as for the melt case.

The equilibrium structure (and, in particular, the radius, R_2) of the corona is determined by a balance between the free energy of "elastic" stretch of B blocks on one side, and excluded volume interactions of B links in the solvent on the other side. The latter interactions tend to swell the corona, while the stretch limits the degree of swelling. As is well-known,[25,46,47] the balance gives rise to the picture of blobs of variable sizes (scaling picture), the energy of the corona being proportional to the total number of blobs. The size ξ of a blob at a distance r from the center can be obtained from the geometrical packing condition:

$$2Q\xi^2(r) = 4\pi r^2$$

where Q is determined by eq 4. Thus

$$\xi(r) = (2\pi/Q)^{1/2} r$$

On the other hand, the blob size (which is simultaneously equal to the correlation length of the solution) is connected with the number of B links per blob, g:

$$\xi = a_B g^{\nu}$$

where $\nu \simeq 0.59 \simeq {}^3/_5$ is the Flory exponent for a flexible polymer coil in a good solvent. Any B block consists of two stretched parts, with the middle point being at the largest distance from the micelle's center. Within the adopted blob picture, any stretched half of a B block can be represented as a completely aligned (along the micelle's radius) sequence of blobs. Thus the number of links in a part $N_B/2$ can be written as

$$N_B/2 = \int_R^{R_2} \frac{dr}{\xi(r)} g(r) = \int_R^{R_2} \frac{dr}{\xi} (\xi/a_B)^{1/\nu} = (2\pi/Q)^{0.5(1/\nu-1)}[(R_2/a_B)^{1/\nu} - (R/a_B)^{1/\nu}]$$

Now we could take into account that $R_2 \gg R$ since soluble blocks are longer and also the corona is swollen (see eq 42). Therefore

$$R_2 \sim a_B N_B{}^{\nu} Q^{0.5(1-\nu)} \tag{37}$$

The free energy of the corona is of the order of kT times the number of blobs;[25,32,46] thus (note that kT is taken as the unit)

$$F_{corona} \sim Q \int_R^{R_2} \frac{dr}{\xi(r)} \sim Q\left(\frac{Q}{2\pi}\right)^{1/2} \ln(R_2/R) \tag{38}$$

Comparing the energies of the core (see eq 5) and the corona, we easily find that the core contribution is always negligible in comparison with the corona:

$$F_{core} \ll F_{corona}$$

provided that $a_A{}^2 \gg \sigma_A$.

Thus the free energy of a micelle can be written as

$$F = F_{intf} + F_{corona} \simeq 4\pi R^2\gamma + Q(Q/2\pi)^{1/2} \ln(R_2/R) \tag{39}$$

An equilibrium state should correspond to the minimum of the free energy per block, F/Q. Using eqs 37–39 after the minimization, we get

$$Q \sim \gamma^{6/5}(N_A v_A)^{4/5}; \qquad R \sim N_A{}^{3/5} v_A{}^{3/5} \gamma^{2/5}$$

$$R_2 \sim a_B N_B{}^{\nu} \gamma^{0.6(1-\nu)} (N_A v_A)^{0.4(1-\nu)} \tag{40}$$

The ratio R_2/R can thus be represented as (we use the numerical value $\nu \simeq {}^3/_5$)

$$R_2/R \sim \frac{a_B N_B{}^{3/5}}{\gamma^{4/25}(N_A v_A)^{11/25}} \tag{41}$$

Here we omit all numerical (and also logarithmic) prefactors.

The largest possible value of the interfacial tension in the SSL, $\gamma = \gamma^*$, is defined below (see eq 43). Using this value, we get the lowest estimate for the ratio R_2/R in the SSL:

$$R_2/R \gtrsim \frac{N_B v_B}{N_A v_A}\left(\frac{\sigma_A}{\sigma_B}\right)^{2/3} \tag{42}$$

Both factors on the right-hand-side of inequality (42) are large (see eqs 1 and 2); therefore the corona size is always larger than the core size in the strong segregation regime.

Geometrical characteristics of micelles, eq 40, are in agreement with the results previously obtained for the same system.[48] Note that the radius of the core, R, is

larger than the Gaussian size of an A block if N_A is large and even if N_A is not large but γ is large enough. Note also that the corona size, R_2, is much larger than the size of a swelled isolated B block, $a_B N_B^{\nu}$. Finally, we see that the equilibrium number of blocks per micelle, Q, is always large (for both large and small N_A) if $\gamma(v_A)^{2/3} \gg 1$.

4.2. Sphere to Disk Transition. As can be seen from eq 40, the size of a spherical micelle increases continuously as the interfacial tension, γ, is increased (we are not going to discuss how to change γ, just assuming formally that γ is changed). However, there is a natural limit for the core radius, R: it cannot be larger than half of the contour length of the (completely extended) A block:

$$R \le R_{max} = N_A a_A/2$$

Using eqs 40, we find that the core size should become of the order of R_{max} for $\gamma \sim \gamma^*$, where

$$\gamma^* \sim N_A a_A/\sigma_A^{3/2} \tag{43}$$

For $\gamma > \gamma^*$ we come to a qualitatively new regime of the micellar structure, the superstrong segregation limit (sSSL), where the core radius levels off at R_{max}.

In the sSSL the most important part of the micellar free energy is its interfacial energy:

$$F_{intf} = \gamma S$$

where S is the total surface area of the core. Thus the energy per block is (for a spherical core of radius $R = R_{max}$)

$$F_{intf}/Q = \gamma S/Q = 3\gamma N_A v_A/R = 6\gamma v_A/a_A \tag{44}$$

It is easy to show that the free energy is smaller for a cylindrical micelle of diameter $2R_{max}$ and for a plane sheet of thickness $2R_{max}$:

$$(F_{intf}/Q)_{cyl} = 4\gamma v_A/a_A; \qquad (F_{intf}/Q)_{plane} = 2\gamma v_A/a_A \tag{45}$$

Therefore it is natural to expect that micelles would change their shape and would transform to planar sheets (disks) or cylinders (see Figure 2b,c).

In order to consider the transition in more detail, we use the model of a spherocylinder or of a disk with rounded edges which was introduced in the previous section. The interfacial free energy of a nonspherical micelle in solution can be calculated in exactly the same way as for the melt case and thus is given by eqs 16 and 20. The corona free energy is given by eq 38, where within the logarithmic approximation the ratio R_2/R under the log can be calculated for a spherical micelle at the expected transition point, i.e., using eq 41 with $\gamma = \gamma^*$. Hence

$$F_{corona} \simeq \text{const} \times Q^{3/2} \ln\left(\frac{a_B \sigma_A^{6/25}}{v_A^{11/25} a_A^{4/25}} \frac{N_B^{3/5}}{N_A^{3/5}}\right) \tag{46}$$

where const is a numerical factor which is irrelevant for what follows. A numerical calculation of thus defined free energy, $F = F_{intf} + F_{corona}$, as a function of the order parameter $D - H$ for prolate and oblate micellar shapes shows that cylindrical micelles in solution are always less stable than disks, in agreement with the results for the melt case. A transition to the disk shape occurs at the very beginning of the sSSL region, at $\gamma = \gamma^*$ given by eq 43, as a second-order transition. The structure of a micelle for $\gamma \gg \gamma^*$ can be described as follows.

The interfacial contribution to the free energy for the disk shape of the core is given by the second equation (45) in a zeroth-order approximation. In addition, we must also take into account the edge contribution to the interfacial area. Thus we get

$$F_{intf}/Q \simeq 2\gamma v_A/a_A(1 + \text{const} \times H/D) = 2\gamma v_A/a_A + \text{const} \times \gamma v_A N_A/D \tag{47}$$

where $H = 2R_{max}$ is the core thickness, D is the diameter of the disk, and const is a numerical factor to be omitted below.

The free energy of the corona for a disk shape can be calculated using eq 38. Omitting the log prefactor, we get

$$F_{corona}/Q \sim D/\sigma_A^{1/2} \tag{48}$$

Equation 48 is valid provided that $D < R_2$, where R_2 is the outer radius of the corona given by eq 37.

The equilibrium disk diameter could now be obtained by minimization of the free energy per chain, $(F_{intf} + F_{corona})/Q$. Thus

$$D \sim \sigma_A^{3/4}(a_A N_A \gamma)^{1/2} \tag{49}$$

The number of blocks, Q, in a disk-shaped micelle is determined by the volume of the core $V_{core} = (\pi/4)D^2H$:

$$Q = V_{core}/(N_A v_A) \sim \sigma_A^{1/2} a_A \gamma N_A \tag{50}$$

The last two equations are valid for $\gamma > \gamma^*$ and for $D < R_2$. These conditions are equivalent to

$$\gamma^{**} > \gamma > \gamma^* \tag{51}$$

where

$$\gamma^{**} \sim (\sigma_B/\sigma_A)^{1/\nu} a_A^{-1} \sigma_A^{-1/2} N_B^{2}/N_A \tag{52}$$

In the region (51), the size of the corona, R_2, is much larger than that of the core, D; the corona in this regime retains its spherical shape whereas the core is disklike (see Figure 2c). Using eqs 37 and 50, we get

$$R_2 \sim a_B(\sigma_A^{1/2} a_A \gamma)^{(1-\nu)/2} N^{(1-\nu)/2} N_B^{\nu} \tag{53}$$

For even larger interfacial tension (or for smaller N_B), $\gamma > \gamma^{**}$, the edge contribution to the interfacial free energy is so unfavorable that the diameter D of the most stable disk-shaped micelle becomes infinite. For a micelle formed by a single multiblock copolymer chain, the diameter is determined by the total number of blocks, Q:

$$Q = N/f; \qquad D = (2N/f\sigma_A/\pi)^{1/2} \tag{54}$$

The structure of a micelle for very large N/f is similar to that shown in Figure 3: the micelle consists of a disk-shaped core surrounded by the disk-shaped corona of thickness

$$H_2 = R_2 \sim a_B(\sigma_B/\sigma_A)^{(1-\nu)/2\nu} N_B \tag{55}$$

The results for the geometrical parameters of associates (micelles) can be summarized as follows:

(a) $\gamma < \gamma^*$, spherical micelles:

$$Q \sim \gamma^{6/5}(N_A v_A)^{4/5}; \qquad R \sim N_A^{3/5} v_A^{3/5} \gamma^{2/5}$$

$$R_2 \sim a_B N_B^{\nu}(N_A^2 v_A^2 \gamma^3)^{(1-\nu)/5} \tag{56}$$

(b) $\gamma^* < \gamma < \gamma^{**}$, disk-shaped core, spherical corona:

$$Q \sim \sigma_A^{1/2} a_A \gamma N_A; \qquad H = 2R_{max} = N_A a_A$$

$$D \sim \sigma_A^{3/4}(\gamma N_A a_A)^{1/2}; \qquad R_2 \sim a_B \times (\sigma_A^{1/2} a_A \gamma)^{(1-\nu)/2} N^{(1-\nu)/2} N_B^{\nu} \tag{57}$$

(c) $\gamma > \gamma^{**}$, disk-shaped core and corona:

$$Q = \mathcal{N}; \qquad H = 2R_{max} = N_A a_A; \qquad D = (2\mathcal{N}\sigma_A/\pi)^{1/2}$$

$$H_2 = R_2 \sim a_B N_B (\sigma_B/\sigma_A)^{(1-\nu)/2\nu} \tag{58}$$

The last two equations (57) are in agreement with the results[49] obtained for disklike micelles formed by rod–coil copolymers in solution.[45]

Note that in the regime (c) the "double spherical layer" type of the associate (which can be obtained by appropriate deformation of the initial large disk) might be more favorable than the plane disk since there is no edge effect for the "spherical layer" (Figure 6). It is interesting to note that the radius of such a spherical layer (which is of the order of D; see eq 58) is proportional to the square root of the molecular weight of a multiblock copolymer chain, i.e., has the same molecular weight dependence as the size of a Gaussian coil.

5. Discussion and Conclusions

We have considered a system of multiblock copolymers with two types of blocks and strong compositional asymmetry ($N_B \gg N_A$). Shorter blocks are assumed to consist of strongly interacting groups (SIGs), which strongly attract each other. In particular, the SIGs might be of ionic nature.

The SIGs aggregate and form multiplets (micelles) if the interaction parameter is large enough. Having in mind the assumed compositional asymmetry, one may expect that the multiplets must be spherical, as in a similar case of block copolymer micelles.[22,24-28] Our main result is that this is not the case provided that the interaction parameter (γ) is high enough and/or the blocks with SIGs are short enough: in the region $\gamma \gtrsim \gamma^*$ it is disklike aggregates that are the most stable. The change of the aggregate's shape (spheres to disks) is shown to be a second-order transition, which occurs as soon as the system can be described by the so-called superstrong segregation limit (sSSL),[37] which implies that the aggregate size approaches the length of a completely stretched minor (A) block.

The tendency for the shape change can be rationalized in simple geometrical terms: for high enough γ it is the energy of the interfaces (the surfaces of the aggregates) that gives the dominant contribution to the free energy of the system. The equilibrium structure of the system corresponds to the minimum of the energy per unit volume, or per block; thus for large γ we need to minimize the interfacial area per block. The areas per block for spherical, cylindrical, and disklike aggregates of the same diameter (thickness in the case of disks) scale as 3:2:1 (see eqs 44 and 45). Therefore disklike or lamellar aggregates are the most favorable. We have also shown that cylindrical aggregates are never stable, even in an intermediate regime.

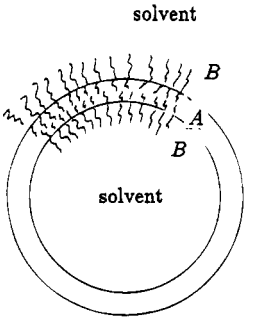

Figure 6. A lamellar micelle transformed into a spherical layer.

If the interaction parameter is further increased, the equilibrium shape of the aggregates changes again from a disk with a finite diameter to an infinite lamellar sheet. This first-order transition occurs at $\gamma^{**} \gg \gamma^*$. It is important to note that although the aggregates (the micellar cores) become fairly asymmetric already in the region $\gamma \gtrsim \gamma^*$, the shape of a micelle as a whole, which is determined by conformations of the major (B) blocks in the corona, remains nearly spherical up to $\gamma \simeq \gamma^{**}$. In the region $\gamma \sim \gamma^{**}$ both core and corona of the micelles become nonspherical (oblate). The schematic dependence of the diameter of the spheres (or disks) on the interaction parameter is shown in Figure 5.

The above general statements are equally applicable both to melts of polymers with SIGs and to their solutions. For both cases the first critical interaction parameter γ^* is proportional to N_A, and the second, γ^{**}, to N_B^2/N_A. Therefore a decrease of the length of strongly interacting blocks (of N_A) could induce a transition from spherical to disklike multiplets and also form infinite lamellae to disks. Note that for a large ratio of N_B/N_A, the region of stability of disklike multiplets is very large since $\gamma^{**}/\gamma^* \sim (N_B/N_A)^2$.

Disklike micelles were also considered theoretically for a different system, rod–coil copolymers.[44] However, a transition from spherical to disklike shape was not studied in this previous paper since rodlike blocks could hardly form a spherical core.

Disklike (as well as tubular) aggregates were also predicted for systems of zwitterionic associating polymers on the basis of detailed numerical calculations taking into account specific interactions between different links.[50] Here a disklike core is formed by relatively small zwitterionic head groups which attract each other via electrostatic (dipole–dipole) interactions. These interactions dictate antiparallel alignment of head groups (dipoles), which is incompatible with a spherical core shape. That is why a sphere to disk (or to another nonspherical micelle) transition had not been considered in ref 50.

Nonspherical aggregates predicted in this paper have been recently observed in melts and solutions of ionomers and associative polymers.[11-16] In particular, disklike[12,13] and lamellar[14] microstructures have been reported. An interesting phenomenon has been observed for an ionomer melt: as ionic content increases, the ion-rich microstructure transforms from a continuous to a discontinuous one.[16] This effect can be explained in the framework of the present theory: increase of the ionic content implies an increase of the

(average) size of the ionic blocks (N_A) and thus an increase γ^*. This might result in a transition from disklike micelles, which could easily form a continuous (or quasi-continuous) phase, to unconnected spherical micelles.

Acknowledgment. The authors are grateful to M. Rubinstein for stimulating discussions. Partial support from E. I. Du Pont de Nemours and Co. and the Russian Foundation of Fundamental Research (RFFI) is acknowledged. This work was completed during a stay of two of the authors (I.A.N. and A.N.S.) in Cavendish Laboratory of Cambridge University. The authors would like to thank Prof. M. Cates and the TCM group for hospitality.

References and Notes

(1) Goodman, I., Ed. *Developments in Block Copolymers*; Applied Science Publishers: New Yor, 1982, Vol. 1; 1985, Vol. 2.
(2) Aggarwal, S. L. *Polymer* **1976**, *17*, 938.
(3) Eisenberg, A. *Macromolecules* **1970**, *3*, 147.
(4) MacKnight, W. J.; Earnest, T. R. *Macromol. Rev.* **1981**, *16*, 41.
(5) Eisenberg, A.; Hird, B.; Moore, R. B. *Macromolecules* **1990**, *23*, 4098.
(6) Gauthier, S.; Eisenberg, A. *Macromolecules* **1987**, *20*, 760.
(7) Weiss, R. A.; Sen, A.; Pottick, L. A.; Willis, S. L. *Polym. Commun.* **1990**, *31*, 220.
(8) Venkateshwaran, L. N.; York, G. A.; DePorter, C. D.; McGrath, J. E.; Wilkes, G. L. *Polymer* **1992**, *33*, 2277.
(9) Moore, R. B.; Bittencourt, D.; Gauthier, M.; Williams, C. E.; Eisenberg, A. *Macromolecules* **1991**, *24*, 1376.
(10) Witten, T. A. *J. Phys. (Fr.)* **1988**, *49*, 1055.
(11) Rebrov, A. V.; Ozerin, A. N.; Svergun, D. I.; Bobrova, L. P.; Bakeev, N. F. *Vysokomol. Soedin.* **1990**, *32A*, 1593.
(12) Hilger, C.; Drager, M.; Stadler, R. *Macromolecules* **1992**, *25*, 2498.
(13) Hilger, C.; Stadler, R. *Macromolecules* **1992**, *25*, 6670.
(14) Lu, X.; Steckle, W. P.; Weiss, R. A. *Macromolecules* **1993**, *26*, 5876.
(15) Lu, X.; Steckle, W. P., Jr.; Weiss, R. A. *Macromolecules* **1993**, *26*, 6525.
(16) Kim, J.-S.; Jackman, J.; Eisenberg, A. *Macromolecules* **1994**, *27*, 2789.
(17) Helfand, E. *J. Chem. Phys.* **1975**, *62*, 999.
(18) Helfand, E.; Wasserman, Z. R. *Macromolecules* **1976**, *9*, 879.
(19) Helfand, E.; Wasserman, Z. R. *Macromolecules* **1978**, *11*, 960.
(20) Helfand, E.; Wasserman, Z. R. *Macromolecules* **1980**, *13*, 994.
(21) Helfand, E.; Tagami, Y. *J. Chem. Phys.* **1972**, *56*, 3592.
(22) Semenov, A. N. *Sov. Phys. MJETP (Engl. Transl.)* **1985**, *61*, 733.
(23) Kawasaki, K.; Ohta, T.; Mitsuharu, K. *Macromolecules* **1988**, *21*, 2972.
(24) Semenov, A. N. *Macromolecules* **1989**, *22*, 2849.
(25) Birshtein, T. M.; Zhulina, E. B. *Polymer* **1989**, *30*, 170.
(26) Birshtein, T. M.; Zhulina, E. B. *Vysokomol. Soedin.* **1985**, *27A*, 1613.
(27) Zhulina, E. B.; Birshtein, T. M. *Vysokomol. Soedin.* **1987**, *29A*, 1524.
(28) Zhulina, E. B.; Semenov, A. N. *Vysokomol. Soedin.* **1989**, *31A*, 177.
(29) Tuzar, Z.; Kratochvil, P. In *Surface and Colloidal Science*; Matijeric, E., Ed.; Plenum Press: New York, 1993.
(30) Halperin, A.; Tirrell, M.; Lodge, T. *Adv. Polym. Sci.* **1992**, *100*, 31.
(31) Fredrickson, G.; Bates, F. *Annu. Rev. Phys. Chem.* **1990**, *21*, 525.
(32) Halperin, A. *Macromolecules* **1987**, *20*, 2943.
(33) Marques, C.; Joanny, J. F.; Leibler, L. *Macromolecules* **1988**, *21*, 1051.
(34) Nagarajan, R.; Ganesh, K. *J. Chem. Phys.* **1989**, *90*, 5843.
(35) Leibler, L. *Macromolecules*, **1980**, *13*, 1602.
(36) Fredrickson, G. H.; Helfand, E. *J. Chem. Phys.* **1987**, *87*, 697.
(37) Nyrkova, I. A.; Khokhlov, A. R.; Doi, M. *Macromolecules* **1993**, *26*, 3601.
(38) Inequalities (1) ensure that the model described below is quantitatively valid. However, these inequalities are not important for *qualitative* conclusions of the paper, which are valid also for the case of comparable sizes of A and B links.
(39) Dreyfus, B. *Macromolecules* **1985**, *18*, 284.
(40) Goin, J. P.; Williams, C. E.; Eisenberg, A. *Macromolecules* **1989**, *22*, 4573.
(41) Williams, D. R. M.; Fredrickson, G. H. *Macromolecules* **1992**, *25*, 3561.
(42) Landau, L. D.; Lifshitz, E. M. *Electrodynamics of Continuous Media*; Pergamon Press: Oxford, London, New York, Paris, 1984.
(43) Alexander, S. *J. Phys. (Fr.)* **1977**, *38*, 983.
(44) Raphael, E.; de Gennes, P.-G. *Physica A* **1991**, *177*, 294.
(45) Note that since A blocks (which fill the micellar core) are almost completely stretched in the superstrong segregation limit, the structure of disklike micelles in this limit is similar to that for micelles formed by rod−coil copolymers with soluble coil parts corresponding to B blocks in our model.
(46) Daoud, M.; Cotton, J. P. *J. Phys. (Fr.)* **1982**, *43*, 531.
(47) Witten, T. A.; Pincus, P. A. *Macromolecules* **1986**, *19*, 2509.
(48) Halperin, A. *Macromolecules* **1991**, *24*, 1418.
(49) Halperin, A. *Macromolecules* **1990**, *23*, 2424.
(50) Bredas, J. L.; Chance, R. R.; Silbey, R. *Macromolecules* **1988**, *21*, 1633.

MA9463876